



HAL
open science

Accurate theoretical predictions on the mechanisms of OSiS formation and its dissociation channels

M. A. M. Paiva, B. Lefloch, B. R. L. Galvão

► **To cite this version:**

M. A. M. Paiva, B. Lefloch, B. R. L. Galvão. Accurate theoretical predictions on the mechanisms of OSiS formation and its dissociation channels. *Monthly Notices of the Royal Astronomical Society*, 2018, 481, pp.1858-1861. 10.1093/mnras/sty2382 . insu-03693514

HAL Id: insu-03693514

<https://insu.hal.science/insu-03693514v1>

Submitted on 13 Jun 2022

HAL is a multi-disciplinary open access archive for the deposit and dissemination of scientific research documents, whether they are published or not. The documents may come from teaching and research institutions in France or abroad, or from public or private research centers.

L'archive ouverte pluridisciplinaire **HAL**, est destinée au dépôt et à la diffusion de documents scientifiques de niveau recherche, publiés ou non, émanant des établissements d'enseignement et de recherche français ou étrangers, des laboratoires publics ou privés.

Accurate theoretical predictions on the mechanisms of OSiS formation and its dissociation channels

M. A. M. Paiva,¹ B. Lefloch² and B. R. L. Galvão^{1*}

¹Departamento de Química, Centro Federal de Educação Tecnológica de Minas Gerais, CEFET-MG Av. Amazonas 5253, 30421-169, Belo Horizonte, Minas Gerais, Brazil

²Univ. Grenoble Alpes, CNRS, IPAG, F-38000 Grenoble, France

Accepted 2018 August 27. Received 2018 August 20; in original form 2018 June 11

ABSTRACT

Multireference configuration interaction calculations are performed to investigate the potential energy surface of the S+SiO and O+SiS reactions, which are of astrochemical relevance. Several singlet and triplet electronic states are calculated in order to explore the reaction paths. It is shown that although collisions with ground-state reactants do not lead to the OSiS molecule adiabatically, the probabilities for such a spin-forbidden process are high. It is also predicted that SiS is easily converted to SiO. Spin orbit couplings and other properties are also calculated and several electronic states are explored.

Key words: astrochemistry – molecular data – ISM: molecules.

1 INTRODUCTION

Since its first detection by Morris et al. (1975), SiS was successfully observed towards the envelope of evolved stars (Cernicharo et al. 2000) and high-mass star-forming regions like Sgr B2 (Dickinson & Kuiper 1981) and Orion KL (Ziurys 1988, 1991; Tercero et al. 2011). Recently, it was detected for the first time in a solar-type star-forming region by Podio et al. (2017). All studies of star-forming regions showed that, similar to the well-studied SiO molecule, SiS is also produced in shock regions.

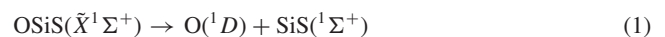
There is strong observational evidence that in quiescent clouds most of silicon is trapped into the dust grains cores and only a few per cent may be stored in the mantles or in gas phase in the form of Si or Si⁺ (Gusdorf et al. 2008b). Under strong shock conditions ($V_s > 25 \text{ km s}^{-1}$) silicon is released in the gas phase in the form of atomic Si and/or SiO, as a result of grain sputtering and/or grain-grain shattering. Silicon is subsequently converted into SiO through reactions of Si with O₂ and OH (Gusdorf et al. 2008a; Guillet et al. 2011). On the contrary, despite its relevance for astrochemical studies, the origin of SiS still remains strongly debated.

Detailed observations of the shock region L1157-B1 at high angular resolution with the IRAM interferometer show that the spatial and velocity distributions of SiO and SiS are different, leading to conclude that both molecules are of chemically different origin.

Currently, the origin and the evolution of SiS in shocks is not understood and the reactions considered in the existing chemical networks such as KIDA¹ are not confirmed experimentally (Wakelam et al. 2015).

In this work, we explore the reaction $\text{SiS} + \text{O} \rightarrow \text{S} + \text{SiO}$ and its reverse, which may provide a clue to the source of SiS and its eventual relation to SiO. The formation of stable OSiS, which is also of astrophysical relevance (Schnöckel 1980; Lefèvre et al. 1998; Thorwirth et al. 2011; Esplugues et al. 2013), is analysed. This species was first observed in gas phase by Thorwirth et al. (2011) and shows a significant dipole moment ($\mu_a = 1.47D$). Although it was not observed in the interstellar medium, Esplugues et al. (2013) have provided an upper limit for its column density in Orion KL. Together with the results of Tercero et al. (2010) the abundance ratio between SiS and OSiS has been estimated as $N(\text{SiS})/N(\text{OSiS}) \geq 22$.

Although OSiS has been investigated theoretically in the context of silicon–oxygen–sulfur oligomers (Krüger 2003; Wang et al. 2005), no attention has been paid to its formation/dissociation. The spin-allowed channels would yield atoms in their first excited states:



while the inverse reaction with ground-state atoms O(³P) or S(³P), would necessarily lead to an energetic triplet state of OSiS, and thus a singlet/triplet crossing must be present in the dissociation path. Such possibilities are analysed in this work.

2 AB INITIO METHODS

The energy calculations here reported used the state-averaged complete active space self-consistent field (CASSCF) method as reference, considering the two lowest electronic states of each calculated symmetry. The full-valence active space consisting of 16 electrons in 12 orbitals was employed, with the aug-cc-pV(X+d)Z (or simply AV(X+d)Z) basis set (Dunning et al. 2001). Geometries were optimized at this level of theory for the lowest electronic state of each

* E-mail: brenogalvao@gmail.com

¹<http://kida.obs.u-bordeaux1.fr/>

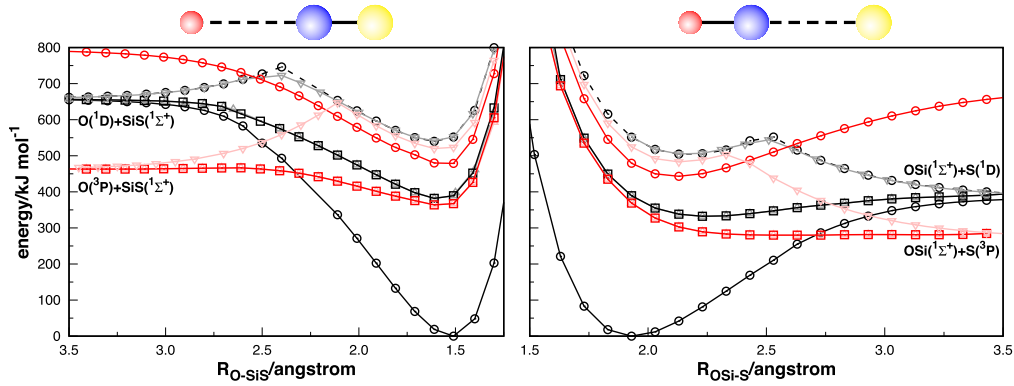


Figure 1. Optimized linear path for atom–diatom collisions leading to OSiS. Singlet states are shown in black/grey while triplet ones are in red/pink. The geometries optimized for the singlet ground state are employed in the calculation of all curves. Energies are at the MRCI/AV($T + d$)/Z level.

calculation. Vibrational frequencies and zero-point energy (ZPE) corrections are also at the CASSCF level. To improve the energy values, each point was refined with multireference configuration interaction method including Davidson correction MRCI(Q) (Werner & Knowles 1988a,b). We have employed the MOLPRO (Werner et al. 2015) package in all calculations.

For obtaining higher accuracy, the final minima and transition states reported were optimized at AV(Q+d)/Z level and the MRCI energies were extrapolated to the complete basis set (CBS). The CASSCF energies were extrapolated with the Karton and Martin protocol (Jensen 2005; Karton & Martin 2006; Varandas 2007)

$$E_X^{CAS}(\mathbf{R}) = E_\infty^{CAS}(\mathbf{R}) + B/X^{5.34}, \quad (3)$$

where X represents the basis sets cardinal number [$X = 3, 4$ for AV(T+d)/Z and AV(Q+d)/Z, while the CBS limit is represented by $X = \infty$]. The variable \mathbf{R} is a vector representing the three interatomic distances, while E_∞^{CAS} and B are parameters to be determined by fitting the equation the *ab initio* results.

The extrapolation of the dynamical correlation (*dc*) was performed according to the USTE method (Varandas 2007), in which the *dc* energy of both basis sets are fitted to

$$E_X^{dc} = E_\infty^{dc} + \frac{A_3}{(X - 3/8)^3} + \frac{A_5^{(0)} + cA_3^n}{(X - 3/8)^5}, \quad (4)$$

where the fitting process provides E_∞^{dc} and A_3 . The parameters $A_5^{(0)}$, c , and n are system-independent and constant for a given post-HF method (Varandas 2007). Their values for MRCI method are $A_5^{(0)} = 0.0037685459 E_h$, $c = -1.17847713 E_h^{1-n}$, and $n = 1.25$ (Varandas 2007).

The probabilities of singlet–triplet transitions are discussed in terms of the magnitude of the spin-orbit coupling (SOC). For this purpose, the full spin-orbit matrix was calculated with the Breit–Pauli operator (Berning et al. 2000) as implemented in MOLPRO (Werner et al. 2015). The spin-free electronic Hamiltonian eigenstates, labelled $|S\rangle$, $|T, 1\rangle$, $|T, 0\rangle$, and $|T, -1\rangle$, are used to build the total Hamiltonian matrix representation ($H_{el} + H_{SO}$). The singlet–triplet spin-orbit transition probabilities will depend on the magnitude of the V_{SO} term, which is defined as

$$V_{SO}^2 = \sum_{M_S=-1}^1 |(T, M_S|H_{SO}|S\rangle|^2. \quad (5)$$

3 RESULTS AND DISCUSSION

3.1 Linear dissociation of OSiS($^1\Sigma^+$)

The minimum energy path for reactions (1) and (2) were calculated for the ground singlet state by separating an atom from OSiS by steps of 0.1 Å, while optimizing the remaining diatomic bond distance and valence angle. At the optimized geometries, several excited states were also calculated and plotted in Fig. 1. This procedure confirmed that the minimum energy path for the OSiS($^1\Sigma^+$) dissociation occurs via linear configurations, and the calculation of all other states were performed at the resulting linear geometry using symmetry (under the C_{2v} point group).

As seen, the adiabatic dissociation to the singlet products occurs without a reaction barrier, and after energy refinement with CBS extrapolations and ZPE corrections, it shows a well depth of $369.4 \text{ kJ mol}^{-1}$ to the dissociation to $S(^1D) + \text{SiO}(^1\Sigma^+)$. Five electronic states must correlate to this asymptotic channel, and it is seen that the first two excited states are degenerate. Since they are not repulsive, they may contribute to $\text{O}(^1D) + \text{SiS}(^1\Sigma^+) \rightarrow \text{SiO}(^1\Sigma^+) + S(^1D)$ exchange reaction.

Crossings between singlet and triplet states are observed during dissociation of OSiS, which could be anticipated, since O and S atoms have triplet ground states. It must be emphasized that Fig. 1 is fixed for linear geometries, following the singlet state minimum energy path. However, the minimum on the crossing seam and collisions in the triplet state follow different paths. The most important features regarding these collisions are shown more accurately in Fig. 2, using fully optimized geometries and MRCI(Q)/CBS energies. To assess the accuracy of our calculations we compare the experimental value for $S(^3P)$ to $S(^1D)$ excitation of $110.5 \text{ kJ mol}^{-1}$ with the difference between singlet and triplet dissociated channels, here calculated as $105.4 \text{ kJ mol}^{-1}$. The comparison shows chemical accuracy, and supports the other results obtained in this work using the same methodology.

3.2 Triplet states

If one is interested in collisions between ground-state reactants, the triplet states must be considered. From Fig. 2 it is readily seen that SiS is easily converted to SiO via reactions with atomic oxygen in its ground state. Our calculations show that this reaction proceeds without any reaction barrier. From an astrophysical point of view, this reaction provides an easy destruction route of SiS in shock regions, when atomic oxygen is released in the gas phase.

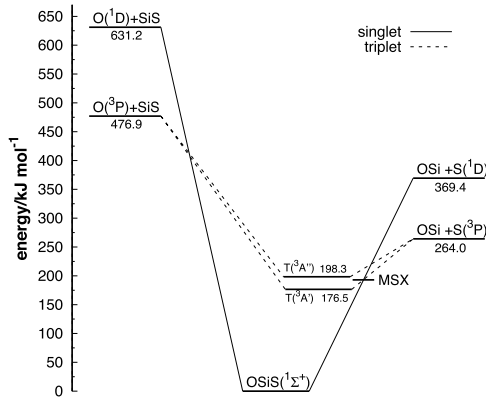


Figure 2. Potential energy profile at the MRCI(Q)/CBS level of theory, including ZPE corrections. The solid lines connecting the structures correspond to the singlet state paths, while the dashed ones are triplet.

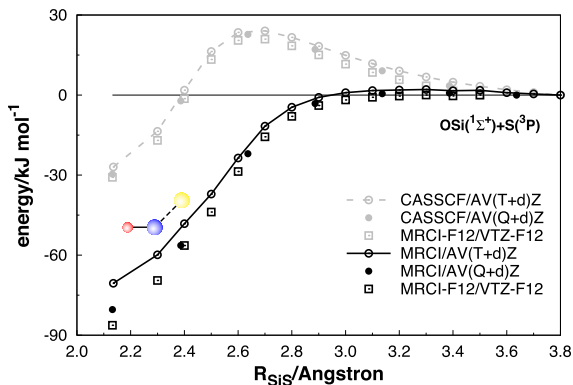


Figure 3. Attack of a ground state S atom into SiO in the ground triplet state (${}^3A'$). CASSCF calculations with different basis are shown in grey, while MRCI are in black. The valence angle and SiO bond length are optimized at each point.

Three electronic states correlate to $S({}^3P) + \text{SiO}({}^1\Sigma^+)$, being the ${}^3A'$ the lowest one. Performing a minimum energy path for this collision (Fig. 3), we observe that it does not occur via linear geometries as the singlet one. It is also seen that the CASSCF approach predicts a small barrier of about $\sim 20 \text{ kJ mol}^{-1}$ for reaction, while inclusion of dynamic correlation effects (with MRCI calculations) and large basis sets tend to remove the barrier. Fig. 3 shows the results with three different basis set. Using the AV(Q + d) Z basis a barrier of

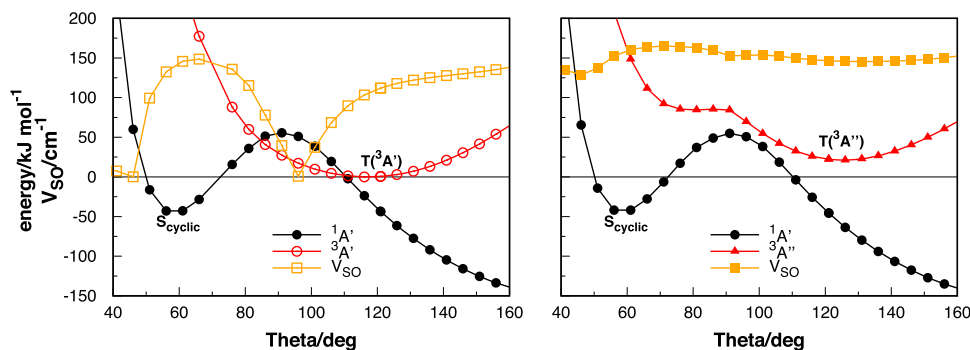


Figure 4. MRCI/AV(T+d)Z bending of the triplet minima (${}^3A'$ in the left-hand panel and ${}^3A''$ in the right-hand panel) with SiS and SiO bond lengths fixed for the corresponding triplet minimum. Energies are given in kJ mol^{-1} relative to $T({}^3A')$, while the spin orbit coupling is given in cm^{-1} .

$\sim 1 \text{ kJ mol}^{-1}$ is predicted to exist, which lies below chemical precision and also less than the expected accuracy of our calculations. Therefore, this collision is likely to occur on a purely attractive potential energy surface (PES).

After a collision takes place in the ${}^3A'$ sheet, a potential well of 87 kJ mol^{-1} is achieved [here denoted $T({}^3A')$], with a bond angle of 121° . Collisions in the ${}^3A''$ sheet are also attractive, achieving a shallower minimum 66 kJ mol^{-1} and a bond angle of 123° [named $T({}^3A'')$].

Although these minima are likely to be achieved barrierlessly, an exchange reaction towards $\text{O} + \text{SiS}$ is very endothermic and unlikely to happen. However, if a triplet OSiS molecule is produced from these collisions it could go through an intersystem crossing (ISC) to achieve the singlet minimum $\text{OSiS}({}^1\Sigma^+)$. In any case, this species would be unstable, and must give off energy to generate a stable molecule. Since three-body collisions are nearly absent in the interstellar medium, this mechanism could occur via radiative stabilization (spontaneous emission), or else at the surface of a dust grain.

Our calculations show that this ISC is very likely to occur, because the singlet and triplet states lie very energetically close in regions close to the triplet minima, as shown in Fig. 4. From this graph it can be seen that there is a surface crossing between the ${}^1A'$ and ${}^3A'$ states occurring less than 3 kJ mol^{-1} above the $T({}^3A')$ minimum, while the ZPE for this state amounts to 11 kJ mol^{-1} . This figure also displays the SOC term (V_{SO}), which is seen to have an appreciable magnitude at the crossing geometry. From the right-hand panel of Fig. 4, it is seen that the bending of $T({}^3A'')$ does not lead to a singlet–triplet crossing, but the magnitude of V_{SO} is much larger, due to the existence of more non-vanishing $\langle T, M_S | H_{SO} | S \rangle$ terms.

After a possible ISC, the system will experience a high energy gradient towards formation of $\text{OSiS}({}^1\Sigma^+)$. Fig. 4 also shows that there is another singlet minimum occurring for cyclic geometries. This and other structures will be discussed in the next section.

3.3 OSSi, SOSi, and other stationary structures

The singlet PES shows three linear isomers (OSiS, OSSi, and SOSi), and a cyclic one (denoted as S_{cyclic}). Their geometric parameters, energies and vibrational frequencies are given in Table 1, while their connections are given in Fig. 5. It can be seen that all isomers are connected to the cyclic one, but the linear ones are not connected among themselves. It can also be seen in Fig. 5 that the S_{cyclic} and linear SOSi isomers lie below the dissociation limit and thus have positive binding energies. Among the two, S_{cyclic} has a deeper potential well ($163.0 \text{ kJ mol}^{-1}$), and larger isomerization barriers

Table 1. Properties of the stationary points of singlet and triplet PESs.^a

	R_{OSi}	R_{SiS}	R_{OS}	E^b	$E(\text{ZPE})^b$	$E(\text{CBS})$	ω_1	ω_2	ω_3	ω_4
OSiS($^1\Sigma^+$)	1.516	1.930	3.446	0.0	0.0	0	606	1279	2471	2527
T($^3A'$)	1.526	2.131	3.201	202.3	172.5	176.5	220	503	1194	–
T($^3A''$)	1.537	2.170	3.273	223.3	193.4	198.3	257	465	1156	–
S_{cyclic}	1.652	2.134	1.877	128.2	98.5	101.0	437	531	948	–
SOSi	1.518	3.346	1.828	270.0	264.7	251.4	340	1226	2207	2223
OSSI	3.426	1.931	1.494	298.3	295.8	296.9	614	1129	2360	2365
TS1	1.566	2.137	2.587	252.2	219.4	230.6	474	742 <i>i</i>	915	–
TS2	1.523	3.116	1.994	298.0	267.5	273.0	343 <i>i</i>	447	1346	–
TS3	2.962	2.044	1.527	332.5	300.7	303.0	172 <i>i</i>	579	986	–
$S(^3P) + \text{SiO}$	1.529			282.3	248.4	264.0	1211	–	–	–
$S(^1D) + \text{SiO}$	1.520			394.7	360.8	369.4	1211	–	–	–
$\text{SiS} + \text{O}(^3P)$		1.959		477.9	441.0	476.9	716	–	–	–
$\text{SiS} + \text{O}(^1D)$		1.944		662.2	625.3	631.2	716	–	–	–

Notes. ^aEnergies are given in kJ mol^{-1} , frequencies (ω) in cm^{-1} , and bond lengths in Angstroms.

^bUsing the AV(Q+d)Z basis set.

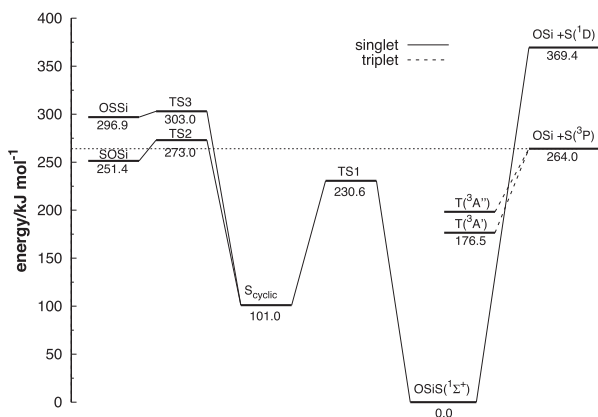


Figure 5. Energy diagram for different isomers and transition states at the MRCI(Q)/CBS level, including ZPE corrections. The dotted line shows the energy of the lowest lying dissociation channel.

(129.6 kJ mol^{-1} towards the global OSiS minimum), and therefore is expected to be more stable. We predict that this structure may also be experimentally obtained. In the triplet states, all linear structures turned out to be transition states leading to the bent triplet minima T($^3A'$) and T($^3A''$).

4 CONCLUSIONS

The potential energy landscape of the OSiS molecule has been explored in depth for several electronic states and using state-of-the-art ab initio methods, proving accurate energetics and mechanism for possible reactions. Among the results, we have calculated that SiS is easily converted to SiO via reactions with atomic oxygen. It is also shown that the formation of OSiS($^1\Sigma^+$) from $S(^3P) + \text{SiO}(^1\Sigma^+)$ collisions may happen under astrochemical conditions, in spite of its spin-forbidden nature. Hence, the detection of OSiS in the interstellar medium with some estimate of its abundance, would bring some useful constraints to this scenario. Several other potential energy features are highlighted and presented.

ACKNOWLEDGEMENTS

The authors would like to thank CAPES, FAPEMIG, and CNPq for the financial support. This work is a collaboration research project

with members of the Rede Mineira de Química (RQ-MG) supported by FAPEMIG (Project: CEX-RED-00010-14).

REFERENCES

- Berning A., Schweizer M., Werner H.-J., Knowles P. J., Palmieri P., 2000, *Mol. Phys.*, 98, 1823
- Cernicharo J., Guélin M., Kahane C., 2000, *A&AS*, 142, 181
- Dickinson D. F., Kuiper E. N. R., 1981, *ApJ*, 247, 112
- Dunning T. H., Peterson K. A., Wilson A. K., 2001, *J. Chem. Phys.*, 114, 9244
- Esplugues G. B., Tercero B., Cernicharo J., Goicoechea J. R., Palau A., Marcelino N., Bell T. A., 2013, *A&A*, 556, A143
- Guillet V., des Forêts G. P., Jones A. P., 2011, *A&A*, 527, A123
- Gusdorf A., Cabrit S., Flower D. R., des Forêts G. P., 2008a, *A&A*, 482, 809
- Gusdorf A., des Forêts G. P., Cabrit S., Flower D. R., 2008b, *A&A*, 490, 695
- Jensen F., 2005, *Theor. Chem. Acc.*, 113, 267
- Karton A., Martin J. M. L., 2006, *Theor. Chem. Acc.*, 115, 330
- Krüger T., 2003, *J. Phys. Chem. A*, 107, 6259
- Lefèvre V., Levillain J., Ripoll J. L., Bailleux S., Bogey M., Wojnowski W., 1998, *Phosphorus Sulfur*, 140, 73
- Morris M., Gilmore W., Palmer P., Turner B. E., Zuckerman B., 1975, *ApJ*, 199, L47
- Podio L. et al., 2017, *MNRAS*, 470, L16
- Schnöckel H., 1980, *Angew. Chem.*, 19, 323
- Tercero B., Cernicharo J., Pardo J. R., Goicoechea J. R., 2010, *A&A*, 517, A96
- Tercero B., Vincent L., Cernicharo J., Viti S., Marcelino N., 2011, *A&A*, 528, A26
- Thorwirth S., Mück L. A., Gauss J., Tamassia F., Lattanzi V., McCarthy M. C., 2011, *J. Phys. Chem. Lett.*, 2, 1228
- Varandas A. J. C., 2007, *J. Chem. Phys.*, 126, 244105
- Wakelam V. et al., 2015, *ApJS*, 217, 20
- Wang R., Zhang D., Liu C., 2005, *Chem. Phys. Lett.*, 404, 237
- Werner H.-J., Knowles P. J., 1988a, *J. Chem. Phys.*, 89, 5803
- Werner H.-J., Knowles P. J., 1988b, *Chem. Phys. Lett.*, 145, 514
- Werner H.-J. et al., 2015, MOLPRO, version 2015.1, a package of ab initio programs
- Ziurys L. M., 1988, *ApJ*, 324, 544
- Ziurys L. M., 1991, *ApJ*, 379, 260

This paper has been typeset from a $\text{\TeX}/\text{\LaTeX}$ file prepared by the author.